J|A|C|S
ARTICLES

Published on Web 05/19/2010

Chemistry under Cover: Tuning Metal−Graphene Interaction by Reactive Intercalation

Peter Sutter,* Jerzy T. Sadowski, and Eli A. Sutter

Center for Functional Nanomaterials, Brookhaven National Laboratory, Upton, New York 11973

Received March 22, 2010; E-mail: psutter@bnl.gov

Abstract: Intercalation of metal atoms is an established route for tuning the coupling of graphene to a substrate. The extension to reactive species such as oxygen would set the stage for a wide spectrum of interfacial chemistry. Here we demonstrate the controlled modification of a macroscopic graphene−metal interface by oxygen intercalation. The selective oxidation of a ruthenium surface beneath graphene lifts the strong metal−carbon coupling and restores the characteristic Dirac cones of isolated monolayer graphene. Our experiments establish the competition between low-temperature oxygen intercalation and graphene etching at higher temperatures and suggest that small molecules can populate the space between graphene and metals, with the adsorbate−metal interaction being modified significantly by the presence of graphene. These findings open up new avenues for the processing of graphene for device applications and for performing chemical reactions in the confined space between a metal surface and a graphene sheet.

Introduction

Graphene, an atomically thin sheet of sp^2-bonded carbon, holds promise for future carbon-based device architectures.[1−3] The interface of graphene with metals is key to realizing large-scale graphene growth,[4−6] forming conventional[7] and spin-polarizing[8] device contacts, and accessing functionalities such as magnetism[9] and superconductivity.[10] For many metals[11] as well as other substrates for graphene epitaxy (e.g., SiC[12]), the strong interfacial interaction with graphene suppresses the characteristic linear π bands that give rise to high-mobility massless Dirac quasiparticles. Efforts to change this interaction have largely focused on intercalation of metal atoms[9,13,14] and recently hydrogen.[15] Here we have used real-time microscopy on monolayer graphene−Ru(0001) to demonstrate the engineering of the interfacial interaction by oxygen. In a wide temperature window, oxygen does not etch graphene but selectively adsorbs on the metal surface beneath the graphene sheet. The complete intercalation of macroscopic domains that are tens of micrometers in size decouples the graphene and restores its linear π bands. The graphene sheet is not merely a passive spectator in this process, but its presence affects the metal−adsorbate interaction. Our findings demonstrate the possibility of performing controlled chemical reactions at the interface with graphene that may be exploited to tune graphene's electronic structure for the fabrication of device elements or to perform selective chemical reactions in the confinement beneath a graphene sheet.

Results and Discussion

Graphene is generally quite inert when exposed to ambient gases such as oxygen at room temperature. At high temperatures, O_2 exposure causes the preferential etching of graphene point defects and edges.[17] These effects become much more pronounced for graphene on metals that facilitate the dissociation of O_2, releasing highly reactive oxygen atoms.[18] Real-time low-energy electron microscopy (LEEM) on epitaxial monolayer graphene on Ru(0001) indeed shows such oxygen etching during O_2 exposure at temperatures above ∼450 °C (Figure 1a,b). An

(1) Novoselov, K. S.; Geim, A. K.; Morozov, S. V.; Jiang, D.; Katsnelson, M. I.; Grigorieva, I. V.; Dubonos, S. V.; Firsov, A. A. *Nature* **2005**, *438*, 197.
(2) Lin, Y.-M.; Jenkins, K. A.; Valdes-Garcia, A.; Small, J. P.; Farmer, D. B.; Avouris, P. *Nano Lett.* **2009**, *9*, 422.
(3) Xia, F.; Mueller, T.; Lin, Y.-m.; Valdes-Garcia, A.; Avouris, P. *Nat. Nanotechnol.* **2009**, *4*, 839.
(4) Sutter, P. W.; Flege, J.-I.; Sutter, E. A. *Nat. Mater.* **2008**, *7*, 406.
(5) Kim, K. S.; Zhao, Y.; Jang, H.; Lee, S. Y.; Kim, J. M.; Kim, K. S.; Ahn, J.-H.; Kim, P.; Choi, J.-Y.; Hong, B. H. *Nature* **2009**, *457*, 706.
(6) Li, X.; Cai, W.; An, J.; Kim, S.; Nah, J.; Yang, D.; Piner, R.; Velamakanni, A.; Jung, I.; Tutuc, E.; Banerjee, S. K.; Colombo, L.; Ruoff, R. S. *Science* **2009**, *324*, 1312.
(7) Lee, E. J. H.; Balasubramanian, K.; Weitz, R. T.; Burghard, M.; Kern, K. *Nat. Nanotechnol.* **2008**, *3*, 486.
(8) Tombros, N.; Jozsa, C.; Popinciuc, M.; Jonkman, H. T.; van Wees, B. J. *Nature* **2007**, *448*, 571.
(9) Varykhalov, A.; Sanchez-Barriga, J.; Shikin, A. M.; Biswas, C.; Vescovo, E.; Rybkin, A.; Marchenko, D.; Rader, O. *Phys. Rev. Lett.* **2008**, *101*, 157601.
(10) Feigel'man, M. V.; Skvortsov, M. A.; Tikhonov, K. S. *Solid State Commun.* **2009**, *149*, 1101.
(11) Giovannetti, G.; Khomyakov, P. A.; Brocks, G.; Karpan, V. M.; van den Brink, J.; Kelly, P. J. *Phys. Rev. Lett.* **2008**, *101*, 026803.
(12) Emtsev, K. V.; Speck, F.; Seyller, T.; Ley, L.; Riley, J. D. *Phys. Rev. B* **2008**, *77*, 155303.
(13) Oshima, C.; Nagashima, A. *J. Phys: Condens. Matter* **1997**, *9*, 1.
(14) Nagashima, A.; Tejima, N.; Oshima, C. *Phys. Rev. B* **1994**, *50*, 17487.
(15) Riedl, C.; Coletti, C.; Iwasaki, T.; Zakharov, A. A.; Starke, U. *Phys. Rev. Lett.* **2009**, *103*, 246804.
(16) Zhou, S. Y.; Siegel, D. A.; Fedorov, A. V.; Lanzara, A. *Phys. Rev. Lett.* **2008**, *101*, 086402.
(17) Liu, L.; Ryu, S.; Tomasik, M. R.; Stolyarova, E.; Jung, N.; Hybertsen, M. S.; Steigerwald, M. L.; Brus, L. E.; Flynn, G. W. *Nano Lett.* **2008**, *8*, 1965.
(18) Starodub, E.; Bartelt, N. C.; McCarty, K. F. Oxidation of Graphene on Metals. 2010, arXiv:1001.4837v2 [cond-mat.mtrl-sci]. arXiv.org e-Print archive. http://arxiv.org/abs/1001.4837v2 (accessed May 14, 2010).

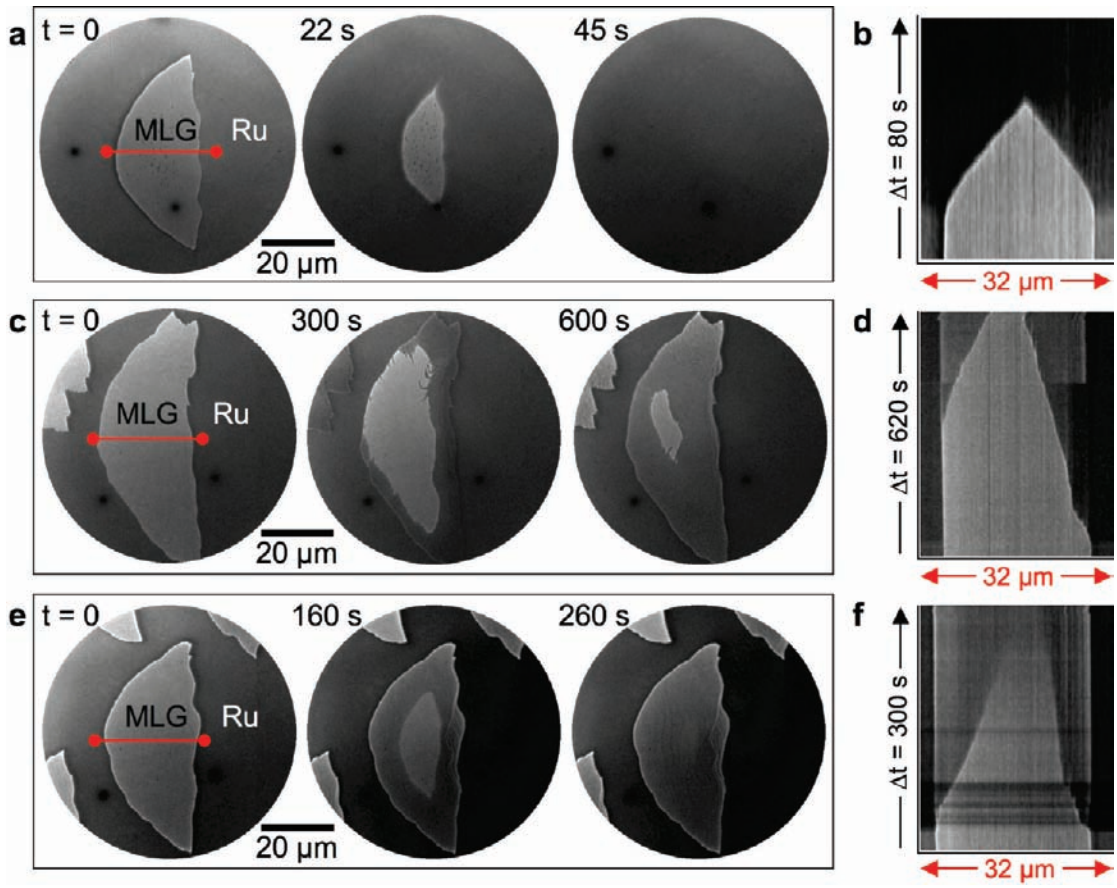

Figure 1. Effects of the exposure of large monolayer graphene domains on Ru(0001) to molecular oxygen and nitrogen dioxide. (a) Sequence of LEEM images obtained during high-temperature O_2 exposure, showing oxygen etching of a graphene domain ($P = 5 \times 10^{-7}$ Torr; $T = 550$ °C). (b) Time-dependent image intensity [$I(x, t)$ map] along the line marked in (a). (c) Low-temperature O_2 exposure, giving rise to oxygen intercalation and selective oxidation of the Ru surface beneath graphene ($P = 5 \times 10^{-7}$ Torr; $T = 340$ °C). (d) $I(x, t)$ map corresponding to (c). (e) Low-temperature NO_2 exposure ($P = 2 \times 10^{-7}$ Torr; $T = 340$ °C). (f) $I(x, t)$ map corresponding to (e). The Ru(0001) substrate steps are aligned approximately vertically in (a), (c), and (e); the uphill direction is from left to right.

initial drop in image intensity within areas of exposed metal that accompanies the adsorption of oxygen on the metal surface[19] is followed by a rapid etching of the graphene edge. The resulting reverse edge-flow continues until no detectable graphene remains on the surface.

When similar graphene domains are exposed to O_2 at lower temperatures (Figure 1c,d), the initial oxygen adsorption on the exposed metal is again followed by changes in image contrast that begin near the edge and extend progressively toward the center of the graphene domain. Throughout this process, however, the modified graphene sheet remains clearly distinguishable from the surrounding metal surface. Below we demonstrate that the observed contrast changes are due to oxygen intercalation (i.e., reaction of the Ru surface with oxygen beneath the intact graphene sheet) accompanied by a decoupling of the originally strongly bound graphene[20] from the metal. Oxygen intercalation during O_2 exposure of graphene on Ru(0001) has been postulated previously on the basis of small-scale scanning tunneling microscopy (STM) combined with photoelectron spectroscopy.[21] The LEEM images shown in Figure 1c,d illustrate that such intercalation is readily scaled up to modify the graphene−Ru interface over macroscopic areas. The front between as-grown and modified graphene is sharply delineated throughout this process, and high-resolution STM shows it to be abrupt on the atomic scale (Supplementary Figure S1). For the lens-shaped monolayer graphene domains on Ru, the intercalation proceeds readily from the straight edge and across substrate steps in the downhill direction but is often hindered at the opposite (rounded) edge of the domain (Figure 1c). Electron microdiffraction on either side of the intercalation front shows a transition from the well-known graphene−Ru(0001) moiré[4] to a structure with additional half-integer diffraction spots, identified as an ordered p(2 × 1) adlayer phase[22] with 0.5 monolayer (ML) of oxygen chemisorbed on the Ru surface beneath the graphene sheet (Supplementary Figure S2).

Exposure to a different oxygen precursor, NO_2, at the same temperature induces similar behavior, namely, the selective modification of the epitaxial graphene monolayer by intercalation. Overall, the intercalation by exposure to NO_2 proceeds substantially faster than that from O_2. It advances uniformly from all edges of the graphene domain. In contrast to the case of O_2, the intercalation front is only initially abrupt and then becomes progressively more diffuse as it propagates from the edge toward the center of the domain (Figure 1e,f).

(19) Madey, T. E.; Engelhardt, H. A.; Menzel, D. *Surf. Sci.* **1975**, *48*, 304.
(20) Sutter, P.; Hybertsen, M. S.; Sadowski, J. T.; Sutter, E. *Nano Lett.* **2009**, *9*, 2654.
(21) Zhang, H.; Fu, Q.; Cui, Y.; Tan, D.; Bao, X. *J. Phys. Chem. C* **2009**, *113*, 8296.
(22) Pfnür, H.; Held, G.; Lindroos, M.; Menzel, D. *Surf. Sci.* **1989**, *220*, 43.

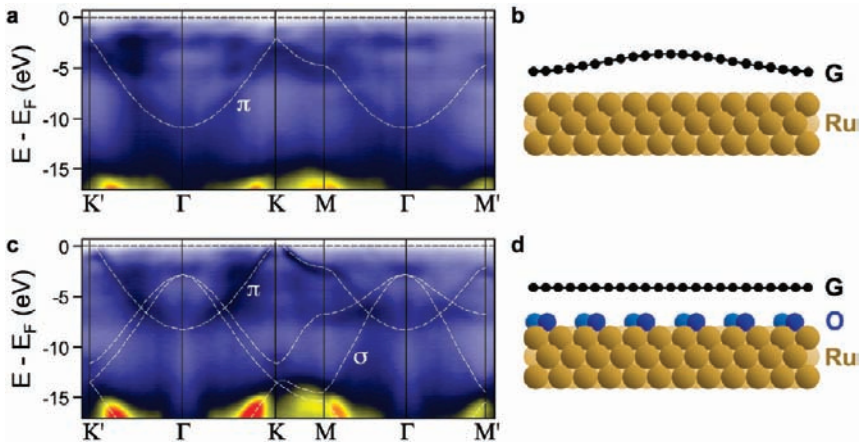

Figure 2. Band structure of monolayer graphene on Ru(0001) before and after oxygen intercalation. (a) Micron-sized spot angle-resolved photoelectron spectroscopy (micro-ARPES) map of the band structure of as-grown monolayer graphene on Ru(0001), reflecting the strong coupling to the metal d states. (b) Schematic of the corresponding moiré structure with alternating strong and weak coupling between graphene and Ru. (c) Micro-ARPES map after exposure to O_2, showing the restoration of linear π bands crossing the Fermi energy and hole doping with a charge-neutrality point 0.5 eV above E_F. (d) Schematic of the decoupled graphene sheet over an ordered Ru(0001)-(2 × 1)-O structure.

Measurements of the projected band structure (Figure 2) provide direct evidence of the dramatic change in the interfacial coupling between graphene and metal caused by the processes shown in Figure 1c−f. For as-grown monolayer graphene on Ru(0001), metal d states hybridize with the occupied graphene π orbitals.[20,23,24] This strong electronic interaction is reflected by a pronounced (∼2 eV) downward shift of the π bands and the opening of a gap between the π and π* states near the Fermi energy, E_F (Figure 2a). O_2 (or NO_2) exposure at temperatures of ∼300 °C fundamentally alters the electronic band structure. In the modified graphene domains, the π−d hybridization is lifted, leading to the appearance of well-defined graphene π bands crossing the Fermi level with linear band dispersion at the (K, K′) points of the Brillouin zone. The observed intense π bands and the weaker σ bands closely match the band structure of free-standing graphene.[25] Similar to previous experiments on low-temperature adsorption of electron acceptors (e.g., NO_2) on the surface of graphene,[16] charge transfer shifts the neutrality point ("Dirac point") to ∼0.5 eV above E_F, thereby inducing a net hole doping of the graphene sheet. The oxygen exposure also affects the (0001) projected band structure of Ru, notably at the zone center, where the occupied band at −2 eV is strongly modified, consistent with O chemisorption on the metal surface beneath the graphene sheet. The formation of a strongly bound, ordered oxygen adlayer structure causes the coupling of Ru 4d with O 2p states;[26] this saturates the metal d states and weakens the interaction with graphene, which is now limited to residual electron transfer from the graphene sheet to the strong acceptors at the metal surface. The STM contrast change across the intercalation boundary, a sharp transition from a strongly corrugated moiré[24,27,28] to a planar sheet with honeycomb structure similar to that found for free-standing graphene,[29] confirms this picture (Supplementary Figure S1).

We performed additional experiments to address the kinetics of oxygen intercalation and graphene etching as well as the reaction mechanism for Ru oxidation beneath monolayer graphene. Real-time LEEM observations during O_2 exposure at different temperatures were used to analyze the competition between intercalation (leading to the selective oxidation of Ru beneath the graphene sheet) and oxygen etching of graphene. Our results, summarized in Figure 3, show that the two processes are thermally activated but follow distinctly different Arrhenius relations. We write the overall reaction rates as $R = fA \exp(-E_A/k_BT)$, where E_A and k_BT denote the activation barrier and thermal energy, respectively, A is the attempt frequency of the rate-determining step, and f is an "efficiency factor" involving the abundance of the reactant (O_2). A fit of this relation to the measured reaction rates gives E_A and the prefactor, fA. For oxygen intercalation, $E_A = 0.38 \pm 0.05$ eV (Figure 3a). A small prefactor, $fA = 10^{10}$ s^{-1}, indicates a low concentration of mobile species arriving at the reaction front. Oxygen etching of the graphene domain involves a larger activation energy, $E_A = 1.1 \pm 0.1$ eV, so it should generally proceed with a lower rate than intercalation. However, the prefactor for oxidative attack (3×10^{15} s^{-1}) is much larger than for oxygen intercalation, reflecting the unrestricted access of reactants (O, O_2) from the exposed metal to the graphene edge. The overall result of this complex reaction kinetics is a competition between the two processes: intercalation dominates at low temperatures, and a transition to oxygen etching occurs for higher temperatures (Figure 3b).

The observed partitioning into two distinct regimes suggests that intercalated graphene should remain stable to temperatures of at least 400 °C. Real-time LEEM during annealing can thus be used to explore the stability of the interfacial oxygen layer and the reversibility of the intercalation process (Supplementary Figure S4). Heating from the intercalation temperature to ∼400 °C causes no changes in the contrast of the free Ru surface,[30] in agreement with previous measurements on O-covered

(23) Brugger, T.; Günther, S.; Wang, B.; Dil, H.; Bocquet, M.-L.; Osterwalder, J.; Wintterlin, J.; Greber, T. *Phys. Rev. B* **2009**, *79*, 045407.
(24) Wang, B.; Bocquet, M.-L.; Marchini, S.; Günther, S.; Wintterlin, J. *Phys. Chem. Chem. Phys.* **2008**, *10*, 3530.
(25) Heske, C.; Treusch, R.; Himpsel, F. J.; Kakar, S.; Terminello, L. J.; Weyer, H. J.; Shirley, E. L. *Phys. Rev. B* **1999**, *59*, 4680.
(26) Reuter, K. In *Nanocatalysis*; Heiz, U., Landman, U., Eds.; Springer: Berlin, 2007.
(27) Marchini, S.; Gunther, S.; Wintterlin, J. *Phys. Rev. B* **2007**, *76*, 075429.
(28) Sutter, E. A.; Acharya, D. P.; Sutter, P. W. *Appl. Phys. Lett.* **2009**, *94*, 133101.
(29) Stolyarova, E.; Rim, K. T.; Ryu, S.; Maultzsch, J.; Kim, P.; Brus, L. E.; Heinz, T. F.; Hybertsen, M. S.; Flynn, G. W. *Proc. Natl. Acad. Sci. U.S.A.* **2007**, *104*, 9209.
(30) Annealing to higher temperatures causes very rapid combustion of the graphene sheet, similar to the observations discussed in ref 15.

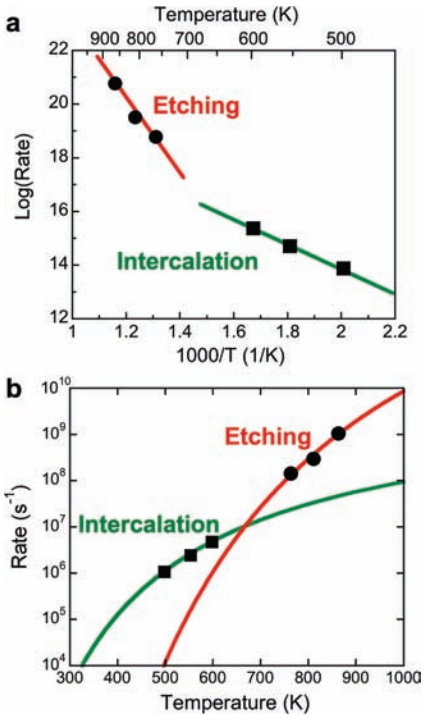

Figure 3. Competition between oxygen intercalation and etching during O_2 exposure of monolayer graphene−Ru(0001). (a) Arrhenius plots showing different activation energies for intercalation (0.38 eV) and etching (1.1 eV). (b) Derived net reaction rates for etching and intercalation, illustrating the branching into two distinct regimes at low and high temperatures.

Ru(0001), which showed recombinative desorption only at temperatures exceeding 530 °C,[19] consistent with a high O binding energy. The contrast of the intercalated graphene domain, on the other hand, changes progressively above an onset temperature of ∼380 °C, reverting from the dark contrast of an intercalated domain to the characteristic bright appearance of as-grown monolayer graphene. On the basis of these observations, we conclude that oxygen intercalation is indeed reversible. Importantly, the presence of graphene affects the binding of oxygen on Ru(0001), weakening the coupling so desorption can occur at temperatures at which O remains strongly bound on the free metal surface.

Our combined experimental findings can be used to shed light on the mechanism of selective Ru oxidation beneath graphene at low temperatures. A comparison of the effects of two different oxygen-carrying precursors, O_2 and NO_2, is an important element of this analysis. O_2 adsorption on bare Ru(0001) is dissociative, initially with a sticking coefficient near unity. At the O_2 pressures used here, it gives rise to a progression of ordered O-adlayer structures, terminating in a p(2 × 1)-O structure at 0.5 ML coverage. At this point, the O_2 sticking coefficient drops sharply, causing an apparent saturation of adsorption.[22] Higher doses do not lead to the continued release of O atoms, but the "excess" O_2 simply desorbs. NO_2 adsorption at elevated temperatures, on the other hand, involves the dissociation to atomic oxygen and NO. The chemisorbed O again forms ordered adlayers, albeit to coverages up to 1 ML. NO desorbs from the free Ru surface at the temperatures considered here.[31]

For Ru(0001) partially covered by monolayer graphene, O_2 exposure at elevated temperatures leads to dissociative adsorption of oxygen on the exposed Ru surface but not on the graphene. Adsorbed O atoms diffuse on Ru(0001), so they can reach the graphene edge and start to decouple the graphene from the metal surface. This process of O_2 dissociation on free Ru and intercalation by O diffusion into areas beneath the graphene domain could in principle continue until the entire graphene sheet is decoupled. If this is the case, the kinetics of O-diffusion on graphene-covered Ru must differ substantially from that on free Ru(0001). Our Arrhenius analysis showed that for graphene intercalation, the activation energy for the reaction-limiting step is $E_A = 0.38$ eV, which is substantially lower than the measured and calculated O diffusion barrier on Ru (0.5−0.7 eV[32,33]). The atomically abrupt intercalation front suggests that the limiting step occurs at the front itself and thus is the decoupling of carbon from the metal. Hence, the diffusion of the intercalating species to the reaction front cannot be the limiting step but must be fast with an activation energy below 0.38 eV. Our de-intercalation experiments indeed show that the presence of graphene weakens the binding of chemisorbed O on Ru(0001), which means that it could similarly reduce the activation energy for O diffusion at the graphene−Ru interface since the diffusion barrier on transition metals scales linearly with adsorbate binding energy.[33]

There is a second possible scenario that may explain the facile oxygen transport between monolayer graphene and Ru: interfacial diffusion could involve a mobile species different from chemisorbed O. Molecular O_2, which is weakly bound to the metal, can be expected to diffuse laterally without significant activation barriers. While on the free Ru surface O_2 either dissociates or desorbs, in the presence of a partially detached graphene sheet that is itself impenetrable to oxygen molecules,[34] the possibility arises that O_2 molecules populate the space between Ru and graphene, diffuse to the reaction front, and dissociate there to drive the continued oxidation of the Ru surface and decoupling of the graphene sheet (Figure 4).

The suggested diffusion of O_2 between the decoupled graphene and the adjacent metal implies that a broader range of chemical reactions involving small molecules could be performed in the confined space between graphene and a metal surface, a concept with far-reaching consequences in surface chemistry and catalysis. Comparing the O van der Waals radius (1.52 Å) and the O_2 bond length (1.21 Å) with the graphene−metal spacing (∼3.3 Å, typical for weakly coupled graphene on metal)[35] indicates that molecular intercalation is indeed plausible. To further corroborate the possibility of intercalation by diatomic molecules, we consider intercalation by NO_2 exposure. Following the initial exposure to NO_2, which causes O adsorption and starts decoupling of the graphene, it again becomes possible for NO molecules to be trapped between graphene and the metal. The activation energy for NO diffusion on Ru(0001) (0.16 eV[33]) is significantly lower than those of the other possible dissociation products (N, 0.94 eV;[36] O, 0.5−0.7 eV[32,33]), so trapped NO could rapidly diffuse to the intercalation front and may become

(31) Stampfl, C.; Schwegmann, S.; Over, H.; Scheffler, M.; Ertl, G. *Phys. Rev. Lett.* **1996**, *77*, 3371.
(32) Wintterlin, J.; Trost, J.; Renisch, S.; Schuster, R.; Zambelli, T.; Ertl, G. *Surf. Sci.* **1997**, *394*, 159.
(33) Nilekar, A. U.; Greeley, J.; Mavrikakis, M. *Angew. Chem., Int. Ed.* **2006**, *45*, 7046.
(34) Bunch, J. S.; Verbridge, S. S.; Alden, J. S.; van der Zande, A. M.; Parpia, J. M.; Craighead, H. G.; McEuen, P. L. *Nano Lett.* **2008**, *8*, 2458.
(35) Sutter, P.; Sadowski, J. T.; Sutter, E. *Phys. Rev. B* **2009**, *80*, 245411.
(36) Trost, J.; Zambelli, T.; Wintterlin, J.; Ertl, G. *Phys. Rev. B* **1996**, *54*, 17850.
(37) Reina, A.; Jia, X.; Ho, J.; Nezich, D.; Son, H.; Bulovic, V.; Dresselhaus, M. S.; Kong, J. *Nano Lett.* **2009**, *9*, 30.

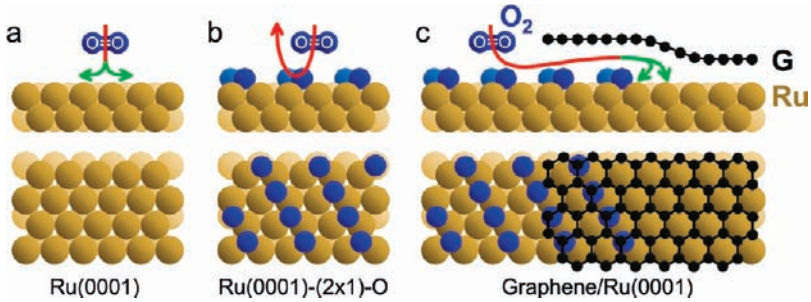

Figure 4. Interaction of molecular oxygen (O_2) with Ru(0001) and monolayer graphene on Ru(0001). (a) Dissociative chemisorption on the clean Ru surface. (b) Saturation of the dissociative adsorption at an oxygen coverage of 0.5 ML in an ordered (2 × 1)-O structure. (c) Molecular intercalation of O_2 beneath monolayer graphene on Ru, leading to simultaneous graphene−metal decoupling and formation of the (2 × 1)-O saturation structure.

the active species controlling the subsequent decoupling of the graphene sheet. While a detailed understanding of this process has yet to be obtained, the presence of nitrogen beneath the graphene sheet would serve as a fingerprint corroborating molecular intercalation. To detect possible N species, we performed ultrahigh-vacuum scanning electron microscopy (UHV-SEM) coupled with nano-Auger electron spectroscopy (nano-AES) (Supplementary Figure S3). UHV-SEM clearly identified the monolayer graphene domains by their characteristic lens shape. While as-grown graphene has a uniform UHV-SEM contrast,[4] graphene domains intercalated from NO_2 show a dark rim surrounding a bright central area. Nano-AES detected oxygen (O_{KLL}) in both regions. There was no detectable N_{KLL} signal in the darker boundary region, but the central brighter area gave rise to additional N_{KLL} lines. Both the core−shell structure of the intercalated graphene domains and the presence of N in the central region are consistent with the intercalation behavior shown in Figure 1e,f and the suggested scenario of a transition from atomic O to molecular NO intercalation during NO_2 exposure. Diatomic molecules such as O_2 or NO can therefore populate the space between weakly coupled graphene and metal and as rapidly diffusing species contribute to the continued decoupling of the graphene sheet (Figure 4).

Conclusions

The complex behavior induced by O_2 or NO_2 exposure of partially graphene-covered Ru(0001) has important implications for the processing of graphene for device applications as well as for transition-metal surface chemistry and catalysis in the presence of graphitic carbon. Growth on transition metals has become one of the leading contenders for large-scale graphene synthesis.[4−6] It is commonly accepted that for applications in electronics, the graphene needs to be transferred from the growth substrate to an insulating support.[5,37] Our observations point to different, possibly simpler processing routes based on selective chemical reactions at the graphene−metal interface. For example, by combining atomic and molecular intercalation of different species (e.g., Si and O_2), it may become feasible to generate thin gate insulators beneath graphene and, following suitable lithographic patterning, to utilize the underlying metal as source, drain, and gate electrodes in a field-effect device.

Our experiments suggest that complex chemical reactions involving both molecular and atomic species may indeed be performed in a controlled way on metal surfaces beneath graphene. This observation contrasts with the long-held notion that graphitic carbon acts as a poison that suppresses desired chemical reactions in surface chemistry and catalysis. The graphene sheet does not merely act as a passive spectator but can provide two types of novel functionality. It generates an extended confined space that can give rise to significant steric hindrance, which should preclude the access of large species and may control the orientation of small molecules. In addition, similar to other strategies (e.g., coadsorption), the presence of the graphene sheet can affect important reaction parameters, such as adsorption energies. Chemistry under graphene covers thus represents a new approach for tuning chemical reactions on transition-metal surfaces.

Acknowledgment. We thank P. Albrecht and D. P. Acharya for performing STM on intercalated graphene, E. Vescovo for technical support, and M. S. Hybertsen for helpful discussions. This work was performed under the auspices of the U.S. Department of Energy under Contract DE-AC02-98CH1-886.

Supporting Information Available: Experimental methods and Supplementary Figures S1−S4. This material is available free of charge via the Internet at http://pubs.acs.org.

JA102398N